RSC Advances

ROYAL SOCIETY
OF CHEMISTRY

www.rsc.org/advances

Table of Contents

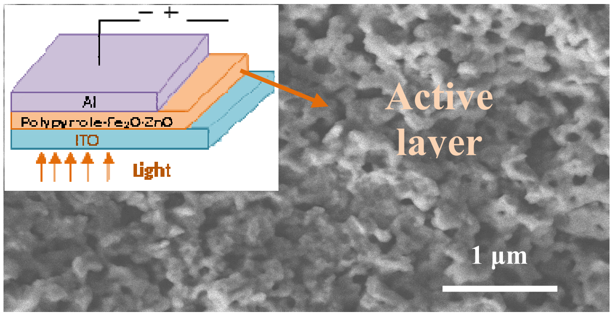

Breakthrough V_{oc} up to >1.5V for polypyrrole-Fe_2O_3ZnO solar-cells is attained from stable dispersions and affected by reactant type and ratio.

Polypyrrole : FeOx·ZnO nanoparticle solar cells with breakthrough open-circuit voltage prepared from relatively stable liquid dispersions

Bao-Yu Zong,*[a] Pin Ho,[b] Zhi-Guo Zhang,[c] Ging-Meng Ng,[†d] Kui Yao,[d] Zai-Bing Guo[e]

[a] *Temasek Laboratories, National University of Singapore, #09-02 TLab Building, 5A Engineering Drive 1, Singapore1174.*

[b] *Department of Materials Science and Engineering, National University of Singapore, 117576, Singapore.*

[c] *Institute of Chemistry, Chinese Academy of Sciences, Zhongguancun North First Street 2, 100190, Beijing, PR China.*

[d] *Institute of Materials Research and Engineering (IMRE), Agency for Science, Technology and Research (A*STAR). 3 Research Link, Singapore 117602. ([†] Now working in Robert Bosch (SEA) Pte Ltd).*

[e] *Core Labs, King Abdullah University of Science and Technology (KAUST), Thuwal 23955-6900, Saudi Arabia.*

***Corresponding author:** Bao-Yu Zong
E-mail: tslzb@nus.edu,.sg
Tel.: + 65-6601 1072, Fax: + 65-6872 6840
Temasek Laboratories,
National University of Singapore,
#09-02 TLab Building, 5A Engineering Drive 1,
Singapore 117411

Abstract

Organic hybrid solar cells with a large open-circuit voltage of up to above that of 1.5 V standard battery voltage was demonstrated by using blends of polypyrrole : $Fe_2O_3 \cdot ZnO$ nanoparticles as the active-layers. The cell active-layers are readily coated in open air from relatively stable liquid dark-color polypyrrole-based dispersions, which are synthesized using appropriate surfactants during in-situ polymerization of pyrrole with $FeCl_3$ or both H_2O_2 and $FeCl_3$ as the oxidizers. The performances of the cells depend largely on the synthesized blend phase, which is determined by the surfactants, oxidizers, as well as the reactant ratio. Only the solar cells fabricated from the stable dispersions can produce both high open-circuit voltage (> 1.0 V) and short-circuit current (up to 7.5 mA/cm^2), due to the relatively uniform porous network nanomorphology and higher shunt to series resistance ratio of the active-layers. The cells also display a relatively high power-conversion efficiency of up to ~3.8%.

Keywords: large open circuit voltage, phase effect, polymer-nanoparticle blend, stable liquid polypyrrole dispersion, porous network active-layer, bulk heterojunction solar cell

1. Introduction

Polymer solar cells (PSCs) are hailed as potential renewable and alternative energy source for electrical power due to their cost-effective preparation, ease and low temperature (< 200°C) processing, as well as ability to produce large area of light active-layer coatings on both flexible and rigid substrates.[1-3] Organic semiconductors also display lower light reflection and higher light absorption coefficient than inorganic semiconductor.[4] Hence if the power-conversion efficiency (ŋ) is largely improved, these “plastic” photovoltaic cells have the potential to become counterparts of inorganic solar cells on commercial markets.[5,6] In recent years, encouraging improvements of ŋ to 3-9% for the organic PSCs have been reported.[5-7] However, more has to be done to further improve the efficiency for the realization of practicable commercial applications.[3,8] Hence finding more suitable ways to increase device efficiency ŋ is required. Since ŋ is proportional to the product of short current (J_{sc}), open circuit voltage (V_{oc}), and field factor (FF), approaches to improve the efficiency involve increasing these components. Most of the progresses made nowadays in device efficiency are based on the improvement of J_{sc} and FF,[6,7] with the largest reported J_{sc} and FF of up to ~20 mA/cm^2 and 85%,[9,10] respectively, for the organic devices. Further increase in FF will be marginal. Furthermore, it is also difficult to improve the J_{sc} significantly as the current density is limited by the intrinsic properties (e.g., charge carrier density, carrier mobility) and structures (e.g., charge transportation channels) of the large molecule-based devices.[11] However, polymers have the potential to produce or bear voltages comparable or higher than inorganic semiconductors.[12] This provides another means for improving the power-conversion efficiency by increasing the V_{oc} while keeping the J_{sc} at a relatively high level. In addition, individual photovoltaic cells with a large voltage (e.g. ≥ 1 V or standard 1.5 V) output also can replace complex multiple cells in unique applications for precise and compact electrical or electronic devices.[13] As such, numerous technical approaches[6,14] are explored to improve V_{oc} by using numerous polymer blends (e.g., poly[2-methoxy-5-(20-ethyl-hexyloxy) and1,4-phenylenevinylene] (MEH-PPV)[15]), in particular, using hybrids of electroactive polymer and inorganic semiconductor (e.g., ZnO, ZnS).[16,17] Despite the significant progresses for improving the V_{oc} to ~1 V, some challenges are still faced, such as the η is still << 1%,[14-17] and the active-layer-coating for these photovoltaic devices usually involved non-air ambience,[18,19] which gives rise to a complex and relatively expensive fabrication process. Therefore, it is demanded to develop an organic solar cell with a large V_{oc} and high J_{sc} through an easy and cost-effective coating process in open air.

In this work, by using $Fe_2O_3 \cdot ZnO$ to replace commonly used pure ZnO for improving the optical property[18,20] and synthesizing relatively stable liquid polypyrrole:$Fe_2O_3 \cdot ZnO$ nanoparticle dispersions to obtain uniform nanostructured porous networks of active-layers, blend PSC cells with a large V_{oc} of up to 1.56 V and a power-conversion efficiency of ~3.8% were demonstrated. The PPy-based dispersions were prepared via the oxidation of pyrrole in the presence of appropriate surfactant stabilizer(s) (e.g., SDBS, PEG, dye, ethanol).

2. Experimental

Preparation of $Fe_2O_3{\cdot}ZnO$ nanoparticles (FZO NP). Zinc acetylacetonate (0.5 mmol), iron(III) acetylacetonate (0.13 mmol), 1,2-hexadecanediol (2 mmol), and benzyl ether (20 ml) were mixed under magnetically stirring, and consequently heated to 200 °C for 2 h and refluxed at 300 °C for 1 h. The mixture was cooled down to room temperature. The black product was precipitated by adding ethanol (40 ml) and separated by centrifugation. The precipitate was then dissolved in hexane in the presence of oleic acid (1.0 mmol) and oleylamine (0.3 mmol), and subsequently precipitated by adding ethanol (25 ml) and centrifuging. The particles were re-dispersed again in hexane according to the ratio of 1 mg : 10 ml. The detailed procedure was similar to that previously reported.[21]

Preparation of stable liquid PPy-based dispersions. Pyrrole [> 98%, C_4H_5N, 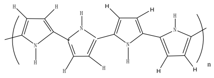, Merck-Schuchardt, Schuchardt, Germany] and surfactants, such as sodium dodecylbenzene sulfonate [SDBS, 80% $CH_3(CH_2)_{11}OSO_3Na$, 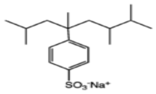, SIGMA Chem. Co., St. Louis, Mo], water-soluble Poly(vinyl alcohol) [PVA, 88% $(C_2H_4O)_x$, 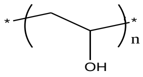, Sigma-Aldrich Company, St. Louis, MO] and PEG [$C_{2n}H_{4n+2}O_{n+1}$, 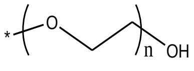,] were used for the preparation of stable aqueous PPy-based dispersions via oxidation. During the preparation, typically a 10 ml of aqueous mixture of pyrrole (0.04 *M*) and the surfactant(s) (e.g., 0.06 *M* SDBS or/and 0.03 *M* other types) were first prepared under vigorous stirring in an ice-bath. The reactant mixture was added gradually into 5 ml of 0.8 *M* H_2O_2 in an ice-bath under vigorous stirring. After stirring for 2 h, the solution was heated to 70-90°C for about 1.5 h until bubbles stopped forming upon the complete decomposition of H_2O_2. It was then cooled to room temperature. 10 ml of 0.4 *M* (or higher) $FeCl_3$ aqueous solution and 1 ml of FZO NP-hexane mixture were consequently added dropwise into the solution. After stirring for about 20 min, the mixture was transferred into an ultrasonic bath where it was stirred for the next 2-20 h to allow the complete evaporation of hexane. Depending on the reactants, the relatively stable dispersions (without or with only a little deposit) ranging from transparent light brown, dark green, to black color were obtained.[3] In the event where only $FeCl_3$ was used as the oxidizer, the addition of H_2O_2 was neglected. The $FeCl_3$, H_2O_2, and other surfactants (without indicating above) were purchased from Sigma-Aldrich Company (St. Louis, MO).

Fabrication and characterization of photovoltaic devices. The indium tin oxide (ITO)-coated glass anodes (20 Ω/sq) were patterned for the easy construction of devices via wet-etching with concentrated HCl as etchant. After patterning, the substrates were pre-cleaned via sequential sonication in deionized water, acetone, and isopropanol for 10 min, respectively, and then dried by N_2 current gas and treated by oxygen plasma for 15 min at 30 W in a plasma machine (Sce106, Anatech USA-SP 100, Hayward, USA). Active-layers, such as from the mixture of PPy·FZO NP dispersion and ethanol (CH_3CH_2OH), water-soluble black dye (Everzol Black B, 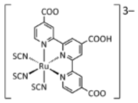

, Everlight Chemical Industrial Corporation, Taiwan), were then prepared by spin-coating on the patterned ITO (anode) surface at a spin speed of 500–2000 rpm. This was followed by slowly drying in a vacuum oven at a temperature of ~40 and 120 °C for 5 and 2 h, respectively. This procedure resulted in 100–250 nm of active-layers. Next, an aluminum (Al) cathode (~200 nm in thickness) was thermally evaporated on each soft-baked film at high vacuum of $1 \sim 3 \times 10^{-4}$ Pa. The photovoltaic cells with an active device area of 0.2 cm^2 were defined using a shadow mask on the film during the Al-electrode deposition, and possessed a structure composing of a blend film of conjugated PPy polymer donor and FZO NP acceptor which were sandwiched between an ITO-positive electrode and Al-negative electrode with a low work function. Finally, the device was removed from the evaporator chamber for testing without protective encapsulation.

The morphologies and thicknesses of the films were measured using a Field Emission Scanning Electron Microscope (FESEM, ELS-7000, Elionix, Japan) with an accelerating voltage of 5-10 kV and a pressure of ≤ 2.8×10^{-4} Pa.[22] The UV-visible absorption spectra were measured on a Hitachi U-3010 UV-vis spectrophotometer. All the UV-signals have been integrated by setting the maximum peak value of the absorbance spectra as 1. The photocurrent density-voltage (J-V) characteristics of the photovoltaic devices, in the dark and under illumination with visible light, were measured on a programmable electrometer (model 238, Keithley Instruments) with AM 1.5G illumination from a Sciencetech solar simulator (model SS150W/SS300W, London, Canada). The measurements were carried out under ambient condition with an intensity of 80 mW/cm^2. During the measurement, the ITO-substrate and Al-film electrodes were correspondingly connected to the positive and negative electrodes of the electrometer analyzer. The series resistance (R_s) of the active-layers was calculated from the inverse slope at $V = V_{oc}$ while the shunt resistance R_{sh} was calculated from the inverse slope at V = 0 in J–V curves under illumination. The conductivity of the active-layers of the photovoltaic devices was examined using four-point-probe method with a Keithley 238 electrometer and power supply. The detailed procedure was similar as our previously reported.[3]

3. Results and Discussion

Organic blend PSCs with the large V_{oc} and relatively high J_{sc} were prepared using the relatively stable liquid PPy-based dispersions with large bandgap, which were synthesized from the oxidation of pyrrole via the 2-step (using H_2O_2 and $FeCl_3$ as the oxidizers consequently) or 1-step (using only $FeCl_3$ as the oxidizer) procedure in the presence of at least one appropriate surfactant.

3.1 Selection of stable PPy-based dispersions for PSC fabrication

Despite much debate over the mechanism governing V_{oc} in organic solar cells,[23] it has been established that large V_{oc} for photovoltaic devices can be obtained using semiconductors of larger bandgaps.[24] Thus, the preparation of PPy polymers was investigated in this work. Although semiconductors with small band gaps have been used as the active-layer to achieve higher J_{sc} by harvesting a larger portion of the solar spectrum, these polymers decreased the V_{oc} value of the devices. PPy-based PSCs possess a high J_{sc} of up to 18 mA/cm^2 and large band gap of 2.0-3.8 eV,[5,25] which are higher than most of the organic semiconductors (e.g., P3HT, polyacetylene, poly(3-octylthiopehene).[16,26] To obtain a larger donor-acceptor interface area, hybrid cells were also fabricated here. From the viewpoint of physical structure for these bulk heterojunction devices, if the reactant (e.g., charge donor and acceptor) components can be evenly dispersed into each other throughout the bulk which results in less exciton lost due to the recombination before dissociation, the bulk heterojunction PSCs can achieve the optimal performance due to the continuous pathways for the holes and electrons to travel through the blend to the electrodes. It is difficult to prepare such blends using conductive polymers in solid or suspension phase (containing much PPy deposit), hence liquid PPy-based dispersions were synthesized in this investigation by using the carefully selected surfactants.

3.2 Selection of surfactant for more stable PPy-based dispersion with optimal performance

Although PPy-based polymers in the solid or suspension phases are usually prepared,[1,27] the PSCs fabricated from the polymers in these phases were below optimal performances. A stable PPy-based dispersion is reported using only H_2O_2 as the oxidizer in the preparation.[28] The performances of the resulted PSCs were poor as well, even using different surfactant(s) (e.g., SDBS, dye, PVA, etc) as the stabilizer(s). This was mainly attributed to the poor absorption of UV-light for these as-synthesized light-color PPy-based blends. The curves (i) and (ii) in Fig. 1a show the low absorption peaks for the blends prepared in the absence and presence of SDBS surfactant, while the J-V curve (i) in Fig. 2a depicts the quite low J_{sc} and V_{oc} of < 0.02 mA/cm^2 and 0.6 V, respectively, obtained for the PSC prepared by using SDBS surfactant. Moreover, some surfactants (e.g., the dye) also led to solid or suspension phase ppy-blends. Hence to improve the PSC performance, H_2O_2 and $FeCl_3$ oxidizers were used consequently via the 2-step oxidation in the synthesis of the PPy-based dispersions. The polymerization changed the dispersions from transparent to dark green or black color (depending on the surfactant type), which significantly increased the UV light absorption in the range of 300–700 nm for the as-synthesized polymers. The curves (iii) and (iv) of Fig. 1a show these improvements in the wavelengths around 400 and 600nm, as well as integration of UV-signals for the polymers prepared in the absence and presence of SDBS surfactant, respectively. With the improved light adsorption, the cell performance (the curve (i) of Fig. 2b) for the blend prepared in the presence of SDBS also increased, with the V_{oc} and J_{sc} values of 1.0 V and 1.2 mA/cm^2, respectively. Further investigation showed that relatively stable dark-color PPy-based dispersions could be synthesized as well using $FeCl_3$ as the only oxidizer in the 1-step oxidation.[3] For the preparations of stable PPy-based dispersions from either the 2-step or 1-step polymerization, suitable surfactant was required to prevent the formation of solid or suspensions with large quantity of deposit in the solution. For instance, the use of SDBS surfactant in the 1-step oxidation also enhanced the stability of the prepared PPy-based blend as little deposits were formed at the bottom of the suspension. The UV light absorption for the as-synthesized blend also improved [Fig. 1b(i)]. To prepare stable PPy-based blends, $Fe_2O_3 \cdot ZnO$ nanoparticles were chosen over commonly used pure ZnO nanoparticles for their better optical property. The FZO NP-hexane was also limited to < 5 ml in the mixture solution. The particles could be readily

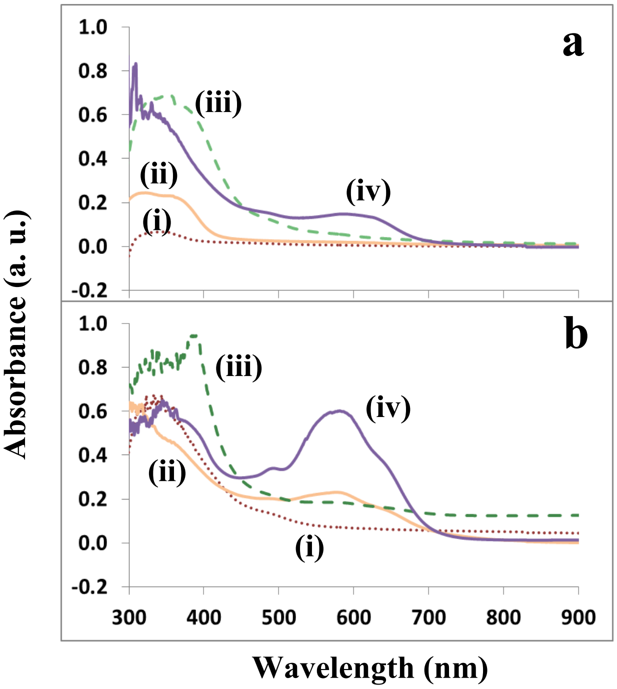

Fig. 1. UV-vis curves of PPy·FNO NP blends prepared from different oxidizers or surfactants. **(a)** By using H_2O_2 oxidizer in the (**i**) absence and (**ii**) presence of SDBS, and by using H_2O_2 and $FeCl_3$ oxidizers in the (**iii**) absence and (**iv**) presence of SDBS. **(b)** By using $FeCl_3$ oxidizer only in the presence of (**i-iv**) SDBS**,** SDBS and PVA, PVA and ethanol, PVA and dye, respectively.

and uniformly doped in the PPy polymers due to the presence of the hydrophilic (-NH_2, -COOH) and hydrophobic [$CH_3(CH_2)_7CH{:}CH(CH_2)_7$-] functional groups from the oleic acid and oleylamine.[21] TEM image [Fig. 3(b) inset] shows that the doped particle size was 5–8 nm. After the stable blends were prepared, the performance of the PSC was further improved by optimizing the surfactant(s). For instance, using other suitable surfactants (e.g., PEG, dye) to replace SDBS in the 2-step oxidization, and using two surfactants in the 1-step oxidation. This optimization also adjusted the composition and improved the stability of the PPy-based blends. Most of the blends formed dispersions, with no or little deposits appearing after being sealed and stored at room temperature for tens of minutes or even several months.

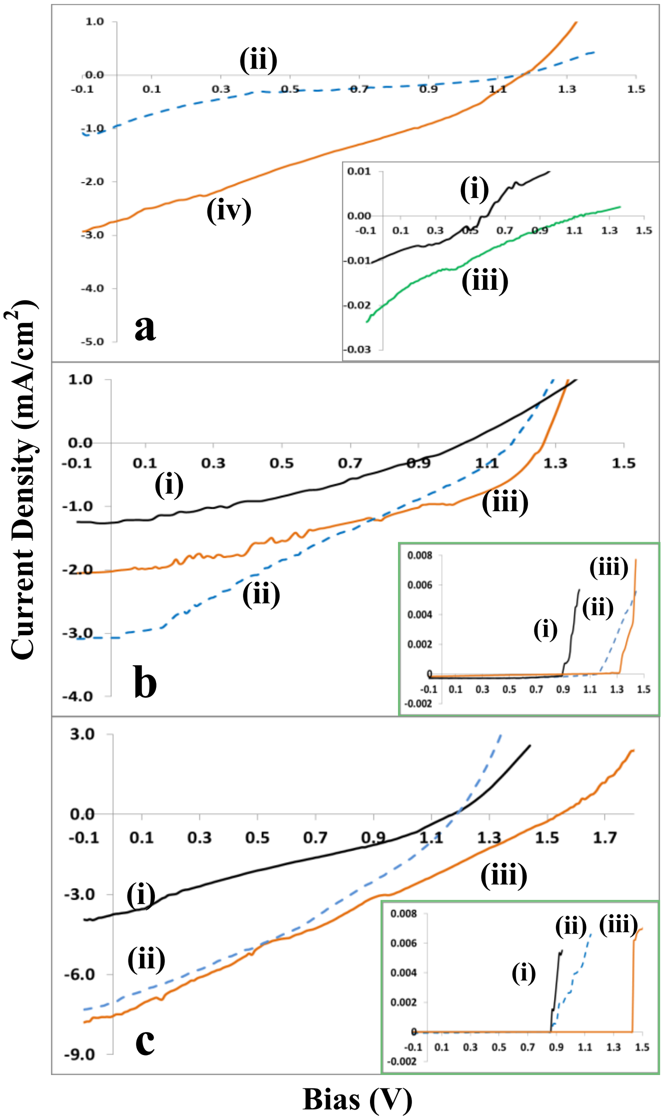

Fig. 2. Current versus voltage (J-V) characteristics of PPy·FZO NP solar-cells, in which Ppy-based blends were prepared from different conditions: by using **(a)** only (**i**) H_2O_2 or (**ii**) $FeCl_3$ in the presence of SDBS; only $FeCl_3$ with (**iii**) high or (**iv**) regular concentration of pyrrole in presence of SDBS and PVA; **(b)** H_2O_2 and $FeCl_3$ in the presence of (**i**) (—) SDBS, (**ii**) (- - -) PEG, and (**iii**) (—) dye. **(c)** only $FeCl_3$ in the presence of (**i**) (—) SDBS and PEG, (**ii**) **(—)** PVA and dye, and (**iii**) (- - -) PVA and ethanol, while the insets in (**b**) and (**c**) represent the corresponding J-V curves under a dark light.

The spectra in Fig. 1b(ii)–(iv) show the improved light absorption for the stable liquid dispersions. In particular, some surfactants (e.g., SDBS and PVA, ethanol and dye) usually produced two peaks of UV light absorption. Therefore, the V_{oc}, J_{sc}, or FF factors of the PPy-based PSCs as-synthesized from the stable dispersions were greatly improved, which were shown in Fig. 2b and c. The J-V curves in Fig. 2b illustrate the effects of different surfactants (e.g., SDBS, PEG, and dye) on the photovoltaic cell performances, in which the PPy active-layers were prepared via the 2-step oxidation. The J_{sc} increased to 1.2-3.1 mA/cm^2 while the V_{oc} improved to the range of 1.0-1.3 V, which were significantly higher than the maximum values (0.50-0.93 V) reported so far for most organic solar cells.[1,5,14,15] Furthermore, the effects of using two surfactants, such as SDBS and PVA, SDBS and dye, and ethanol and PVA were also investigated during the 1-step oxidation polymerization. The curves in Fig. 2(iv) and 2c(i)-(iii) show that the complex surfactants significantly improved the performance of the prepared photovoltaic cells, compared to that from single SDBS surfactant [shown in Fig. 2a(ii)]. In particular, a breakthrough V_{oc} of 1.56 V was achieved, which was higher than standard battery voltage of 1.5 V and almost twice those of most organic photovoltaic cells reported thus far. A high J_{sc} of 6.2 mA/cm^2 was also attained for the photovoltaic cell prepared from the relatively stable PPy-based dispersion in the presence of PVA and ethanol surfactants. A power-conversion efficiency of 3.8% was achieved as well. The improved performance for this PSC compared to other PSCs was due to its relatively highest density and widest UV light absorption [Fig. 1b(iii)]. Thus, suitable surfactant(s) in the reactants improved the stability and light absorption of the PPy-based dispersions, consequently enhancing the performances of the photovoltaic cells. Notably, as the ITO-substrate and Al-film electrode of the PSCs were connected to the positive and negative electrodes of the electrometer, respectively, the illuminating currents measured were usually negative in value and the J-V curves were located at the fourth quadrant of coordinate axis. The kink appeared in the J–V curve was properly associated with the carrier accumulation, which altered the distribution of electric field inside the device. The unbalance of charge carrier mobility, defects or dipoles at the interface, energy barriers and low surface recombination rate of the cathode, etc, are also the plausible reasons for the appeared kink.[29] For the reproducibility of the high V_{oc} and other properties, more results from batches of PSCs revealed that besides the suitable reactants

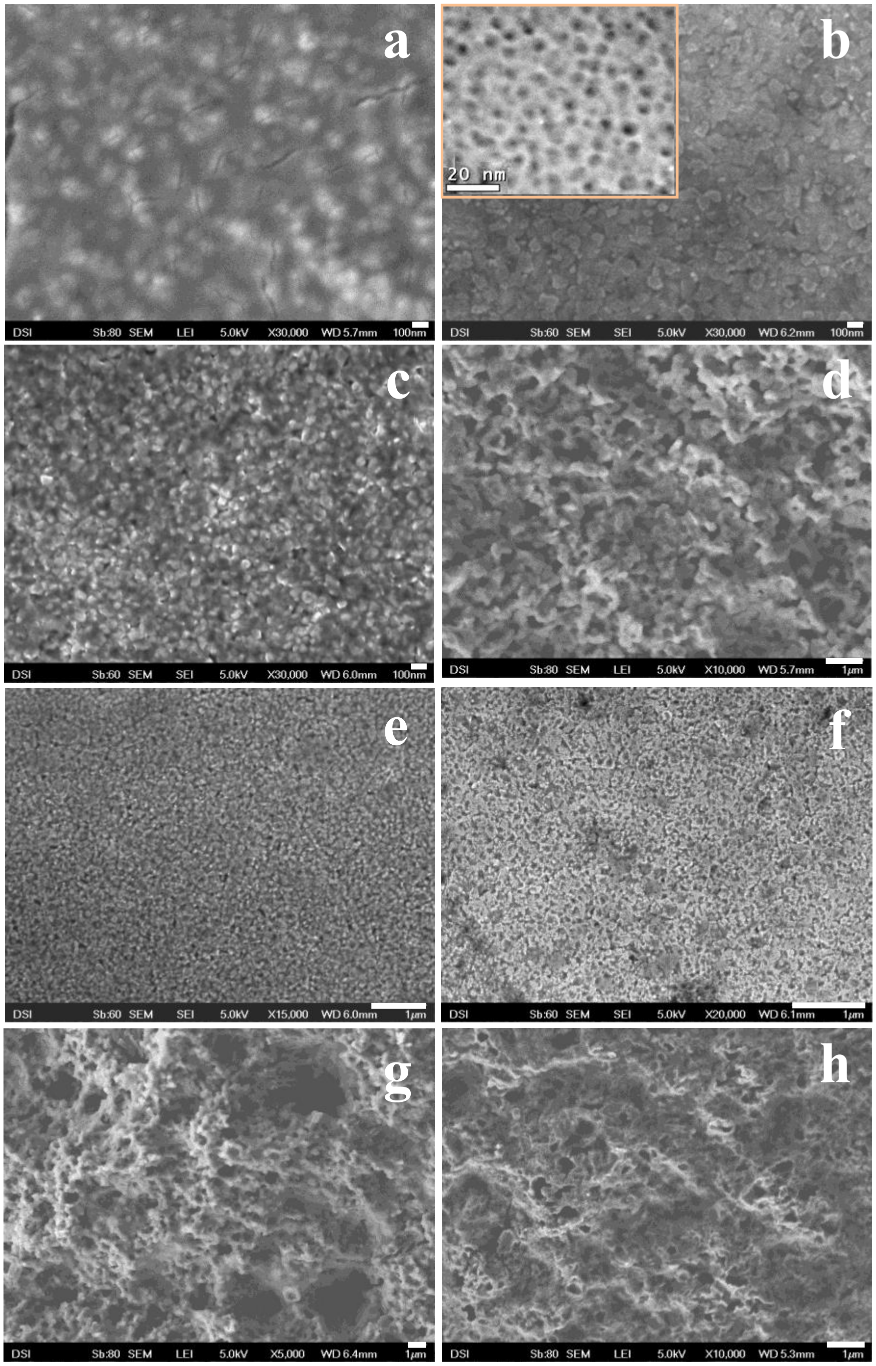

Fig. 3. FESEM images of PPy active-layers prepared from different reactants, mainly containing: **(a)** $FeCl_3$ and SDBS; **(b)** greater or **(c)** regular pyrrole concentration, $FeCl_3$, SDBS and PVA; **(d)-(f)** H_2O_2, $FeCl_3$, and SDBS or dye or PEG, respectively; **(g)** and **(h)** $FeCl_3$, PVA and dye or PVA and ethanol, respectively. The inset of (b) is the TEM image (scale bar: 20 nm) of doped $Fe_2O_3 \cdot ZnO$ nanoparticles in the PPy polymer. The scale bars in the FESEM images are 100 nm for (**a**-**c**) while 1 μm for (**d**-**h**).

and their ratios, the fabrication process (e.g., soft baking, etc) was also crucial. After the active-layer was uniformly coated on an ITO substrate, the subsequent drying process should be carefully controlled. At initial drying procedure for the coated liquid dispersion film, the temperature should be controlled at ~40˚C for at least 5 hours for slowly removing all volatiles in the film. Then the drying temperature could be gradually increased to 120˚C and the baking was kept till the PPy was polymer completely dried. Too short time or too high temperature (e.g., > 60°C) at the initial baking and too high increasing rate (e.g., > 2°C/minute) for the subsequent baking temperature would cause nano-/micro-cracked or pelt film (due to the quickly accumulated internal stress), instead of an even compact active-layer. The film with a cracked morphology or pelt layer consequently led to the poorer performance or reproducibility of the PSC, which will be elaborated in the followings.

3.3 Root causes of physical phase effect of PPy·FNO NP blend to the PSC performance

The above investigations showed that with the selection of suitable different oxidizers or surfactants to produce stable PPy-based dispersions, PSCs were achieved with larger V_{oc}, higher J_{sc} as well as FF, which was difficult to be attained with the PSCs prepared from solid or suspension PPy blends. This phenomenon was further verified with PSCs prepared from the PPy·FNO NP suspension and dispersion. These two blends were prepared from the same reactants (e.g., pyrrole, $FeCl_3$, SDBS, PVA) of different compositional ratios. During syntheses of the PPy-based blend, if the addition of pyrrole was too high (e.g., > 0.1 M in the first mixture solution), the prepared blend was a suspension (instead of stable dispersion) and contained lots of precipitates. The performance comparison for the two different PSCs, prepared from the suspension and dispersion blends, was illustrated in Fig. 2a(iii) and (iv), respectively. The PSC from the suspension displayed almost non-photovoltaic property, whereas the PSC fabricated from the stable PPy-based dispersion possessed a V_{oc} of 1.18 V and a J_{sc} of 2.7 mA/cm^2. This dispersion was prepared utilizing a regular concentration of pyrrole (< 0.08 M in the first mixture solution during the blend preparation), As such, the phase of the blends significantly influenced the performance of the synthesized photovoltaic cells, and the phase could be determined by both the types and ratios of the reactants. This phenomenon is attributed to the fact that different physical phases of the blends affected the coating uniformity, internal structures, and nanomorphologies of the active-layers. Due to fluidity of PPy-based polymers, the liquid dispersions not only allowed large area (e.g., on 6” ITO substrate) of thin stable active-layer to be prepared readily by spin- or blade-coating in open air at room temperature, but also produced relatively uniform porous-network structures after slowly drying. This coating quality is much better than those from the suspensions. The FESEM image in Fig. 3(a) shows the poorer surface morphology of a PSC active-layer fabricated from the suspension by using $FeCl_3$ oxidizer and SDBS surfactant. Fig. 3(b) and (c) show the comparison of the two active-layers prepared from the suspension and dispersion of the same reactants (pyrrole, $FeCl_3$, SDBS, PVA). The active-layers [Fig. 3(a) and (b)] prepared from the two suspensions with different components were flat nano-crack films, which contained bloc-shape components without uniform porous networks. Conversely, the active-layers fabricated with the dispersions, either from the 2-step oxidation using H_2O_2 and $FeCl_3$ or 1-step oxidation using $FeCl_3$, were compact nanoporous 3-dimensional networks without nano-cracks. The pore size varied with the blend compositions. Fig. 3(c)-(i) show the morphologies of the active-layers prepared from different dispersions using different oxidizers and surfactants. Thus, the different nanomorphologies of the active-layers largely influenced the UV light absorption and performance of the PSCs. For the uniform porous network films, the relative intensity and spectrum range of UV light absorption were improved significantly, as the changed components as well as more UV photons were confined within the pores of the film instead of being reflected away. Therefore, the porous nanomorphology partially compensated the narrow light adsorption spectra due to the large band-gap of PPy polymer. As a result, the uniform porous nanostructures led to the improved performance of the photovoltaic cells (Fig. 2b and c). In addition, the chemical stability of the PPy-based polymers ensured that the performances of the solar cells did not deteriorate over time. For example, the J-V curves in Fig. 2(c) show the three PSCs, which were stored in a dry box for three weeks after the preparation, still performed the similar results compared the PSC in Fig. 1(iv), which was also prepared from $FeCl_3$ oxidizer but measured as soon as the completion of its fabrication.

Table 1. Properties of the PPy active-layers prepared from different blends.

Blend	**Oxidizer used**	**Surfactant used**	**R_s** (Ω)	**R_{sh}** (Ω)	**R_{sh}/R_s**	**J_{sc}** (mA/cm^2)	**V_{oc}** (V)	**FF** (%)	**η** (%)
Dispersion	H_2O_2	-	2.0 x10^4	2.2 x10^4	1.1	0.02	0.28	36.0	0.0
Suspension	H_2O_2, $FeCl_3$	-	9.8 x10^2	1.2 x10^2	0.1	0.49	0.98	30.6	0.1
Dispersion	H_2O_2	SDBS	2.2×10^4	6.0×10^4	3	0.01	0.58	23.5	0.0
Suspension	$FeCl_3$	SDBS	5.5×10^2	4.3×10^2	0.8	0.9	1.15	12.5	0.2
Suspension	$FeCl_3$ (much Py)	SDBS, PVA	6.8×10^4	3.1×10^4	0.5	0.02	1.11	12.8	0.0
Dispersion	$FeCl_3$	SDBS, PVA	1.5×10^2	5.2×10^2	3	2.7	1.18	28.5	1.1
Dispersion	H_2O_2, $FeCl_3$	SDBS	3.1×10^2	3.4×10^3	11	1.3	1.04	33.0	0.5
Dispersion	H_2O_2, $FeCl_3$	PEG	75	1.7×10^3	23	3.1	1.16	26.9	1.2
Dispersion	H_2O_2, $FeCl_3$	Dye	81	2.0×10^3	25	2.0	1.28	38.0	1.2
Dispersion	$FeCl_3$	SDBS, PEG	1.2×10^2	4.5×10^2	4	3.8	1.18	25.3	1.4
Dispersion	$FeCl_3$	PVA, Dye	55	3.2×10^2	6	7.1	1.20	32.0	3.4
Dispersion	$FeCl_3$	PVA, ethanol	1.3×10^2	6.2×10^2	5	7.6	1.56	25.5	3.8

Furthermore, the different reactants and their respective molar ratios also determined the conductivity, shunt resistance R_{sh}, and series resistance R_s of the active-layers. The data in Table 1 shows the physical properties of the PSCs prepared with different conditions. The conductivity of the active-layers fabricated from the dispersions was ~0.86 $\Omega\cdot cm^{-1}$, much larger than that (~10^{-3} $\Omega\cdot cm^{-1}$) from most of the PPy-based suspensions with lots of precipitates. This suggested that the charge mobility of the active-layers prepared from the liquid dark-color dispersions was much higher than that from the suspensions. Furthermore, the PPy·FNO NP blends prepared from the stable dispersions have larger R_{sh} and lower R_s, therefore higher R_{sh}/R_s ratio as compared to the blends prepared from the suspensions. As representing the ohmic-loss due to the diode leakage currents from recombination and pinholes in the photovoltaic device,[30] the shunt resistance R_{sh}, which does not contribute to the diode, should be high as possibly to minimize the current leakage. Since the nano-crack and non-uniform component active-layers gave rise to low R_{sh} (shown in Table 1), the PSCs prepared from the suspensions were poor in performance. Moreover, the series resistance R_s of the active-layer represents the ohmic-loss at the surface of cell. Despite not directly contributing to the V_{oc}, the R_s should be small to prevent the exponential diode from increasing to infinitely large current and minimize electrical power loss,[1,30] which is caused by the resistance limiting the current in the device. Thus, a small R_s and high R_{sh} (viz., a high R_{sh}/R_s ratio) will greatly improve the V_{oc} and other performances. Therefore, due to the higher R_{sh}/R_s ratios, the PPy-based PSCs prepared from the relatively stable dark-color dispersions displayed the larger V_{oc} and better performance, contrary to those fabricated from most PPy suspensions.

Although the large V_{oc} of ≥ 1.0 V (Fig. 2) has been attained in most of our prepared PPy PSCs, the FF factor and J_{sc} are lower than some reported PPy-dye sensitized solar cells.[5,18] This is due to the relatively lower conductivity for the synthesized PPy-based blends, which limited the charge mobility. This issue will be addressed in our next development phase.

4. Conclusions

In summary, we have demonstrated an approach of preparing organic photovoltaic devices with large breakthrough open-circuit voltage of 1.65 V by using relatively stable liquid dark-color PPy-based dispersion as the active-layer. Suitable surfactants behaved as stabilizers in the preparation of these stable dispersions and modified the property and morphology of the active-layers, hence the field factor, short circuit current, and open circuit voltage of the PSC devices were significantly improved. Although the efficiency of the prepared solar cells was not comparable with commercial requirement, this preparation method revealed a potential way to achieve improved power-conversion efficiency for practical use.

References

1 P. Würfel, *Physics of Solar Cells: From basic principles to advanced concepts*. John Wiley & Sons, 2009.

2 R. J. Komp, J. Perlin, *Practical photovoltaics: Electricity from solar cells*. 3rd Ed., Aatec Publications, 1995.

3 B. Y. Zong, P. Ho, S. C. Wuang, *Mater. Chem. Phys*. 11 October 2014, Published online http://www.sciencedirect.com/science/article/pii/S0254058414006403.

4 Q. F. Zhang, E. Uchaker, S. L. Candelaria, G. Z. Cao, *Chem. Soc. Rev*., 2013, **42**, 3127-3171.

5 B. E. Hardin, H. J. Snaith, M. D. McGehee, *Nature Photon*., 2012, **6**, 162-169.

6 G. J. Zhao, Y. J. He, Y. F. Li, *Adv. Mater*. 2010, **22**, 4355–4358.

7 J. D. Servaites, S. Yeganeh, T. J. Marks, M. A. Ratner, *Adv. Funct. Mater*. 2010, **20**, 97–104.

8 C. S. Ferekides, D. L. *Morel. Process development for high V_{OC} CdTe solar cells*. Subcontract Report NREL/SR-5200-51605. University of South Florida Tampa, Florida, May 2011.

9 D. J. Burke and D. J. Lipomi, *Energy Environ. Sci.*, 2013, **6**, 2053-2066.

10 W. Tress, K. Leo, M. Riede. *Adv. Funct. Mater*. 2011, **21,** 2140–2149.

11 M. Wright, A. Uddin, *Solar Energ. Mat. Sol. C*. 2012, **107**, 87-111.

12 J. Rostalski, D. Meissner, *Solar Energ. Mat. Sol. C.*, 2000, **63**, 37-47.

13 M. Taguchi, A. Terakawa, E. Maruyama, M. Tanaka. *Prog. Photovolt: Res. Appl.*, 2005, **13**, 481–488.

14 H.Y. Chen, J. H. Hou, S. Q. Zhang, Y. Y. Liang, G. W. Yang, Y. Yang, L. P. Yu, Y. Wu, G. Li, *Nature Photon.*, 2009, **3**, 649-653.

15 M. Bredol, K. Matras, A. Szatkowski, J. Sanetra, A. Prodi-Schwab, *Solar Energ. Mat. Sol. C*. 2009, **93**, 662–666.

16 H. l. YIP, A. K. Y. Jen, *Energy Environ. Sci.* 2012, **5**, 5994-6011.

17 A. Duarte, K. Y. Pu, B. Liu, G. C. Bazan, *Chem. Mater*., 2011, **23**, 501–515.

18 M. GrÄtzel, *Acc. Chem. Res*., 2009, **42**, 1788–1798.

19 E. J. W. List, C. H. Kim, J. Shinar, A. Pogantsch, G. Leising, W. Graupner, *Appl. Phys. Lett*. 2000, **76**, 2083-2085.

20 M. Açıkgöz, M. D. Drahus, A. Ozarowski, J. van Tol, S. Weber, E. Erdem, *J. Phys.: Condens. Matter* 2014, **26**, 1558031-1558039.

21 B. Y. Zong, G. C. Han, Y. K. Zheng, L. H. An, T. Liu, K. B. Li, J. J. Qiu, Z. B. Guo, P. Luo, H. M. Wang, B. Liu, *Adv. Funct. Mater*., 2009, **19**, 1-7,.

22 B. Y. Zong, J. Y. Goh, Z. B. Guo, P. Luo, C. C. Wang, J. J. Qiu, P. Ho, Y. J. Chen, M. S. Zhang, G. C. Han, *Nanotech*.**,** 2013, **24**, DOI: 10.1088/0957-4484/24/24/245303.

23 W. J. Potscavage, A. Sharma, B. Kippelen, *Accounts Chem. Res*., 2009, **42**, 1758-1767.

24 V. Shaktawat, N. Jain, R. Saxena, N. S. Saxena, T. P. Sharma, *J. Optoelectron. Adv. M.*, 2007, **9**, 2130-2132.

25 O. A. Andreeva, L. A. Burkova, M. A. Smirnov, G. K. El'yashevich, *Polymer Sci. (B*), 2006, **48**, 331-334.

26 E. J. W. List, C. H. Kim, A. K. Naik, U. Scherf, G. Leising, W. Graupner, J. Shinar, *Phys. Rev. B*, 2001, **64**, 155204-155215.

27 J. Nelson, *The Physics of solar cells (Properties of semiconductor materials).* Imperial College Press, 2003.

28 V. Bocchi, L. Chierici, G. P. Gardini, *Tetrahedron*, 1970, **26**, 4073–4082.

29 W. Tress, A. Petrich, M. Hummert, M. Hein, K. Leo, M. Riede, *Appl. Phys. Lett.* 2011, 98, 063301-063303.

30 S. Yanagina, Y. H. Yu, K. Manseki, *Accounts Chem. Res*., 2009, **42**, 1827-1838.